

# A model independent measure of the large scale curvature of the Universe

Edvard Mörtzell,<sup>a</sup> Jakob Jönsson<sup>a,b</sup>

<sup>a</sup>The Oskar Klein Centre for Cosmoparticle Physics, Department of Physics,  
Stockholm University, AlbaNova University Center, S-106 91 Stockholm, Sweden

<sup>b</sup>Department of Physics, Oxford University,  
Denys Wilkinson Building, Keble Road, Oxford, OX1 3RH, UK

E-mail: [edvard@fysik.su.se](mailto:edvard@fysik.su.se), [jacke@fysik.su.se](mailto:jacke@fysik.su.se)

**Abstract.** Cosmological distances as a function of redshift depend on the effective curvature density,  $\Omega_K$ , via the effect on the geometrical path of photons from large scale spatial curvature and its effect on the expansion history,  $H(z)$ . Cosmological time, however, depends on the expansion history only. Therefore, by combining distance and lookback time observations (or other estimates of the expansion history), it is possible to isolate the geometrical curvature contribution and measure  $\Omega_K$  in a model independent way, i.e., free from assumptions about the energy content of the universe.

We investigate two different approaches to accomplish this task; the differential and the integral approach. The differential approach requires, in addition to distances, derivatives of distance with respect to redshift as well as knowledge of the expansion history. The integral approach is based on measuring the integral of the inverse of the expansion history via measurements of cosmic time as derived, e.g., from galaxy ages.

In this paper, we attempt to constrain the large scale curvature of the Universe using distances obtained from observations of Type Ia supernovae together with inferred ages of passively evolving galaxies and Hubble parameter estimates from the large scale clustering of galaxies. Current data are consistent with zero spatial curvature, although the uncertainty of  $\Omega_K$  is of order unity. Future data sets with on the order of thousands of Type Ia supernovae distances and galaxy ages will allow us to constrain the spatial curvature  $\Omega_K$  with an uncertainty of  $\lesssim 0.1$  at the 95% confidence level.

**Keywords:** supernova type Ia - standard candles, baryon acoustic oscillations

*Dedicated to Lasse O'Månsson, the late editor-in-chief of Svenska Mad.*

---

## Contents

<b>1</b>	<b>Introduction</b>	<b>1</b>
<b>2</b>	<b>Disentangling cosmic curvature and expansion history</b>	<b>3</b>
2.1	Differential approach	4
2.2	Integral approach	5
<b>3</b>	<b>Observable quantities</b>	<b>5</b>
3.1	Measuring $D(z)$ and $D'(z)$	5
3.2	Measuring $E(z)$	6
3.3	Measuring $I(z)$	7
3.4	Differentiation of data	8
3.5	Integration of data	9
<b>4</b>	<b>Data</b>	<b>9</b>
4.1	Type Ia supernovae	9
4.2	Galaxy ages	9
4.3	Other probes of the Hubble parameter	10
<b>5</b>	<b>Results</b>	<b>10</b>
5.1	Differential approach	10
5.2	Integral approach	10
<b>6</b>	<b>Future</b>	<b>12</b>
6.1	Differential approach	13
6.2	Integral approach	15
<b>7</b>	<b>Summary and Discussion</b>	<b>16</b>
<b>A</b>	<b>Lookback time and galaxy ages</b>	<b>18</b>
<b>B</b>	<b>Derivation of error in the integral approximation</b>	<b>19</b>

---

## 1 Introduction

Current observational evidence is consistent with the universe being made up of  $\sim 5\%$  baryonic matter,  $\sim 25\%$  non-baryonic dark matter, and  $\sim 70\%$  dark energy in the form of vacuum energy, or equivalently, a cosmological constant [1, 2]. In this concordance model, the total energy density is very close to the critical energy density needed for the universe to have zero spatial curvature on large scales. Considerable effort is put into probing the expansion history of the universe in greater detail in order to pinpoint the properties of the dominant dark energy component. Also, there are many ongoing experiments aiming at observing the dark matter at particle level. Less energy is being put into investigating the large scale geometry of the universe.

Most inflationary models predict that the spatial curvature should be on the order of  $|\Omega_K| \lesssim 10^{-5}$  (though there are models that allow for larger curvature) [1, 3]. As such, probing geometry at the largest scales can probe fundamental physics.

Traditionally, the angular size of the fluctuations in the cosmic microwave background (CMB) has been regarded as the most effective way to constrain spatial curvature. The common explanation is that for a fixed physical size of the fluctuations, when compared to the case of a flat geometry, positive curvature (i.e.,  $\Omega_K < 0$ ) will cause the observed angle to be larger and negative curvature ( $\Omega_K > 0$ ) smaller. However, since the relation between the physical scale and the observed angle is given by the angular diameter distance, not only spatial geometry but also the expansion history will affect the observed angle. Specifically, the reason why the observed angle is not as sensitive to the matter density (as expected for a fixed physical scale) is that the physical scale has a very similar dependence on the matter density as the angular diameter distance and thus will be factored out when calculating the observed angle. However, a non zero  $\Omega_K$  affects both the spatial curvature and the expansion rate. Since some of the sensitivity of the CMB observations is due to the effect on the expansion rate, dark energy properties may also affect the observed angular scale of the fluctuations. Conversely, if the spatial curvature of the Universe is non zero, it can mimic evolving dark energy [4–7]. Because of this degeneracy, measurements of the curvature parameter,  $\Omega_K$ , usually involve a parameterised description of the dark energy. Recent measurements of  $\Omega_K$ , utilising combinations of different cosmological probes and simple parameterisations of the dark energy equation of state, indicate that the Universe is nearly flat [8–16]. However, some parameterisations allow large deviations from a flat Universe [17]. The relation between expansion and curvature is also evident from how current bounds on the acceleration depends on curvature [18].

The observed scales of CMB fluctuations are sensitive to the combination  $H_0^2 \Omega_K$ , where  $H_0$  is the Hubble constant. Assuming that the dark energy is in the form of a cosmological constant and incorporating Hubble Space Telescope (HST) priors on  $H_0$ , Wilkinson Microwave Anisotropy Probe (WMAP) 5-year data [1] gives  $-0.2851 < \Omega_K < 0.0099$  at 95% confidence level (CL). If data from baryon acoustic oscillations (BAO) and Type Ia supernovae (SNe Ia) are also included, the limit improves to  $-0.0181 < \Omega_K < 0.0071$ . With the latest WMAP 7-year data [16], these limits change only marginally to  $-0.0133 < \Omega_K < 0.0084$ .

Barenboim et al. [8] investigate how future BAO and CMB data can be used to resolve the degeneracy between curvature and the dark energy equation of state, within a parameterised model for  $w(z)$ . In [3], it is shown how  $\Omega_K$  can be measured with high precision using future CMB data combined with distance observations out to redshifts where the energy content of the universe is dominated by matter. The distance measures can break the degeneracy between  $\Omega_K$  and  $\Omega_M$ , and are less sensitive to the late time dark energy properties. It was shown in [19] how future observations of the growth of structure in the universe could be used to constrain the expansion history and thus, together with distance measurements from CMB and SNe Ia, can constrain  $\Omega_K$  to sub-percent accuracy. A method to probe the purely geometrical part of  $\Omega_K$  using weak gravitational lensing and BAO was devised in [20]. Note that, in contrast to the methods described in [3, 8, 19], this technique is completely independent of the expansion history of the universe and thus to the dark matter and dark energy densities and properties. This is also true for the methods described in this paper, utilising data at lower redshifts. As such, they earn their merit as independent probes of spatial curvature even though they will not be able to compete with the (parameterised) constraints on  $\Omega_K$  from CMB observations.

In section 2 we outline the expansion history independent methods employed in this paper. These methods rely upon observable quantities introduced in section 3. We use the available data, described in section 4, to obtain constraints presented in section 5. In section 6, future constraints on  $\Omega_K$  are investigated using simulated data sets. The results are discussed and summarised in section 7.

## 2 Disentangling cosmic curvature and expansion history

In a Friedmann-Lemaître-Robertson-Walker (FLRW) universe, the expansion history at late times when the contribution from radiation can be neglected, is given by

$$E(z) \equiv \frac{H(z)}{H_0} = [\Omega_M(1+z)^3 + \Omega_K(1+z)^2 + \Omega_{DE}f(z)]^{1/2}, \quad (2.1)$$

where  $\Omega_M$ ,  $\Omega_K$  and  $\Omega_{DE}$  are the current (effective) energy densities of matter, spatial curvature and dark energy, respectively, in units of the current critical density. In terms of the equation of state parameter,  $w(z)$ , the function governing the evolution of the dark energy with time is

$$f(z) = \exp\left(3 \int_0^z \frac{1+w(x)}{1+x} dx\right). \quad (2.2)$$

The parameterisation of the expansion history plays, however, no role in our method. Let us now define the quantity

$$I(z) \equiv \int_0^z \frac{dx}{E(x)}, \quad (2.3)$$

which is proportional to the proper distance. We will make use of the  $H_0$ -independent comoving distance

$$D(z) \equiv \frac{1}{\sqrt{-\Omega_K}} \sin\left[\sqrt{-\Omega_K} I(z)\right], \quad (2.4)$$

which is related to luminosity and angular diameter distances,  $d_L$  and  $d_A$ , through

$$D(z) = \frac{H_0 d_L(z)}{(1+z)} = H_0 d_A(z)(1+z). \quad (2.5)$$

We note that distances depend on the spatial curvature,  $\Omega_K$  in two ways; it affects the expansion rate of the Universe as well as the geometrical path of photons. Any effect on the expansion can be mimicked by a dark energy component with equation of state  $w = -1/3$ , corresponding to  $f(z) = (1+z)^2$ . We therefore seek to isolate the purely geometrical effect of curvature.

The importance of not relying on any assumptions about the expansion history can be appreciated by noting that we do not need very elaborate dark energy models to mimic the effects from spatial curvature on distances out to moderate redshifts. There is an almost perfect degeneracy in distances already between a constant dark energy equation of state parameter,  $w_0$ , and the curvature,  $\Omega_K$ . In figure 1, we show how the observed magnitude of a source changes with redshift and cosmological parameters. We have used a parameterisation of the dark energy equation of state given by

$$w(z) = w_0 + w_1 \frac{z}{1+z}. \quad (2.6)$$

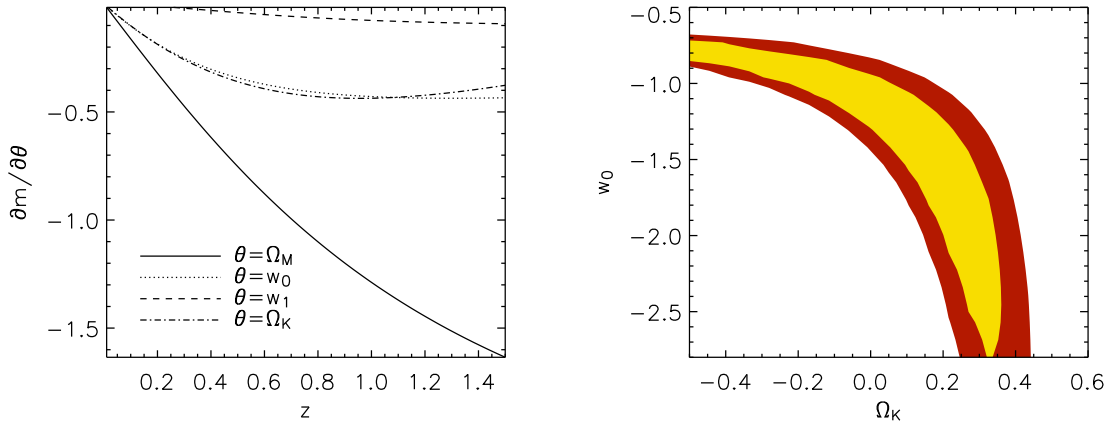


**Figure 1.** *Left panel:* The sensitivity of the observed SN Ia magnitudes to different cosmological parameters  $\theta = \{\Omega_M, w_0, w_1, \Omega_K\}$  as given by the derivatives  $\partial m / \partial w_0(z)$ ,  $\partial m / \partial \Omega_K(z)$  etc. The cosmology is  $\Omega_M = 0.3$ ,  $\Omega_K = 0$ ,  $w_0 = -1$ ,  $w_1 = 0$ . *Right panel:* Contours at the 68.3 and 95% CL in the  $[w_0, \Omega_K]$ -plane from SN Ia observations. This is for the Union2 data set described in section 4.1 assuming a fixed matter density  $\Omega_M = 0.3$  and  $w_1 = 0$ .

Since the shapes of  $\partial m / \partial w_0$  and  $\partial m / \partial \Omega_K$  are very similar, confidence contours from the redshift-distance relation for SNe Ia (here we use the Union2 compilation of SN data described in section 4.1) have a very degenerate structure when fitting for  $\Omega_K$  and  $w_0$ , even for fixed values of  $\Omega_M$  and  $w_1$ . In a similar analysis using SDSS-II SN data [2], a non zero curvature is preferred when using the MLCS2k2 light curve fitter and assuming that dark energy is in the form of a cosmological constant [21].

Note that we assume that the spatial curvature is constant throughout space. This would not be the case in, e.g., so called Lemaître-Tolman-Bondi models. However, it can be shown that in such models, when combining SN Ia data and CMB data, the observer need to be uncomfortably close to the center, thus violating the Copernican principle [22]. We also assume isotropy, i.e., that the universe looks the same in all directions since neither the CMB nor SNe Ia show any deviations from this simple picture [23].

From eq. (2.4), it is clear that (luminosity and angular diameter) distances are degenerate with respect to curvature and expansion history. This degeneracy can be broken if the information from distance measurements is supplemented by the expansion history,  $E(z)$ , or the integral,  $I(z)$ . Two different approaches to measure  $\Omega_K$  can therefore be pursued.

## 2.1 Differential approach

The *differential* approach, originally outlined in [6], is based on differentiating eq. (2.4). We can then write

$$\Omega_K = \frac{(ED')^2 - 1}{D^2}, \quad (2.7)$$

where primes denote derivatives with respect to redshift. This is the curvature contribution to the geometry only; the curvature contribution to the expansion velocity is divided out by  $E(z)$ . The differential approach requires not only distances, but also derivatives of distances as well as independent estimates of  $E(z)$ .

Since  $\Omega_K$  is constant for any FLRW model, eq. (2.7) measured at different redshifts would also offer a test of the Copernican principle [24]. Similar consistency relations for the concordance model, i.e. a flat cosmological constant dominated universe, can be formed by combining  $E(z)$ ,  $D(z)$  and its first and second derivatives [25].

## 2.2 Integral approach

Measurements of the integral  $I(z)$  allows the *integral* approach to be followed. To gain insight into the relation between cosmic curvature, distance, and  $I(z)$  we can study a Taylor expansion of eq. (2.4) around a flat universe

$$D \simeq I + \frac{1}{6}\Omega_K I^3 + \frac{1}{120}\Omega_K^2 I^5 + \mathcal{O}(\Omega_K^3). \quad (2.8)$$

The distance  $D$  is to first order equal to  $I$  and  $\Omega_K$  determines the magnitude of the higher order terms. Neglecting terms of order three and higher in eq. (2.8) leads to a second order equation with the solution

$$\Omega_K \simeq \frac{10}{I^2} \left\{ \sqrt{1 + \frac{12}{10} \left[ \frac{D}{I} - 1 \right]} - 1 \right\}. \quad (2.9)$$

The accuracy of this approximation decreases for increasing redshift. At  $z = 0.5$ ,  $1.0$ , and  $1.5$  the error for  $|\Omega_K| < 0.3$  is smaller than 1, 2, and 6 parts in  $10^5$ , respectively.

## 3 Observable quantities

In the previous section we described how the differential and integral approach can be used to measure the large scale curvature of the Universe in a model independent way. We now discuss how  $D(z)$ ,  $D'(z)$ ,  $E(z)$ , and  $I(z)$  can be obtained from observable quantities.

### 3.1 Measuring $D(z)$ and $D'(z)$

The apparent magnitude,  $m$ , of a SN Ia with absolute magnitude  $M$  is related to the distance  $D$  through

$$m = M + 5 \log \left( \frac{d_L}{\text{Mpc}} \right) + 25 \equiv \mathcal{M} + 5 \log (1 + z) + 5 \log D, \quad (3.1)$$

where

$$\mathcal{M} \equiv M + 5 \log \left( \frac{c/H_0}{1 \text{ Mpc}} \right) + 25. \quad (3.2)$$

This can be rewritten as

$$m - \mathcal{M} = \frac{5}{\ln 10} [\ln (1 + z) + \ln D]. \quad (3.3)$$

Consequently, the derivative of  $m$  with respect to redshift is

$$m' = \frac{5}{\ln 10} \left[ \frac{1}{(1 + z)} + \frac{D'}{D} \right]. \quad (3.4)$$

These two relations can be inverted to yield an explicit formula for the distance,

$$D = \frac{1}{1 + z} \exp \left[ \frac{\ln 10}{5} (m - \mathcal{M}) \right], \quad (3.5)$$

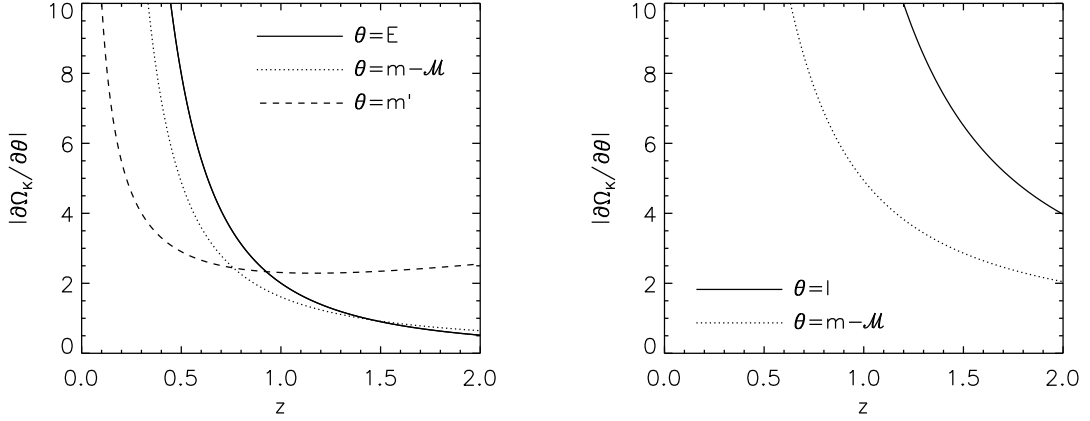


**Figure 2.** *Left panel:* Sensitivity of curvature computed using the differential approach to different observables  $\theta = \{E, m - \mathcal{M}, m'\}$ . A high value indicates that the observed quantity, e.g.  $E(z)$  is not very sensitive to the curvature and we expect the error of  $\Omega_K$  to be large. *Right panel:* Sensitivity of curvature computed using the integral approach to the observables  $\theta = \{I, m - \mathcal{M}\}$ . The underlying cosmology was for both plots assumed to be  $\Omega_M = 0.3$  and  $\Omega_\Lambda = 0.7$ .

and its derivative,

$$D' = D \left[ \frac{\ln 10}{5} m' + \frac{1}{(1+z)} \right], \quad (3.6)$$

in terms of observable quantities. We can now rewrite eq. (2.7) as

$$\Omega_K = E^2 \left[ \frac{\ln 10}{5} m' - \frac{1}{(1+z)} \right]^2 - (1+z)^2 \exp[-0.4 \ln 10 (m - \mathcal{M})], \quad (3.7)$$

i.e.,  $\Omega_K = \Omega_K(E, m - \mathcal{M}, m')$ . If we can measure  $E$ ,  $m - \mathcal{M}$ , and  $m'$ , we can thus constrain the spatial curvature. The error on  $\Omega_K$  is given by

$$\sigma_{\Omega_K} = \sqrt{\left( \frac{\partial \Omega_K}{\partial E} \sigma_E \right)^2 + \left( \frac{\partial \Omega_K}{\partial (m - \mathcal{M})} \sigma_{m - \mathcal{M}} \right)^2 + \left( \frac{\partial \Omega_K}{\partial m'} \sigma_{m'} \right)^2}. \quad (3.8)$$

In the left panel in figure 2 we show how the sensitivity of  $\Omega_K$  to the observables,  $\theta = \{E, m - \mathcal{M}, m'\}$ , varies with redshift, assuming a flat cosmological constant universe with  $\Omega_M = 0.3$ . We expect uncertainties in  $E$  to dominate at low redshifts and uncertainties in  $m'$  to dominate at  $z \gtrsim 1$ . Note that, since  $\Omega_K$  is constant, we can combine data at different redshifts when constraining the global value of  $\Omega_K$ .

### 3.2 Measuring $E(z)$

One way to measure  $E(z)$  is to use the evolution of lookback time with redshift. The  $H_0$ -independent lookback time to an object at redshift  $z$  is given by

$$\tau(z) \equiv H_0(t_0 - t_z) = \int_0^z \frac{dx}{(1+x)E(x)}. \quad (3.9)$$

By differentiating eq. (3.9) and rearranging terms, it is clear that the expansion history can be obtained by differentiation of the lookback time [26],

$$E(z) = -\frac{1}{(1+z)} \frac{dz}{d\tau}. \quad (3.10)$$

In appendix A, the relationship between lookback time and galaxy age is discussed. According to eq. (A.4), the following equality holds

$$\frac{d\tau}{dz} = -H_0 \frac{dt_{\text{age}}}{dz}, \quad (3.11)$$

implying that the evolution of galaxy age,  $t_{\text{age}}(z)$ , with redshift can be used to measure the expansion history.

### 3.3 Measuring $I(z)$

Galaxy ages can also be used to measure the integral (2.3). Taking the derivative of eq. (3.9), rearranging terms and then integrating, we arrive at

$$I(z) = \int_0^z \frac{d\tau}{dz} (1+x) dx = \tau(z)(1+z) - \int_0^z \tau(x) dx, \quad (3.12)$$

where integration by parts was used in the last step. Substituting galaxy ages for lookback times in eq. (3.12) comes at a price; an unknown constant  $T$  enters in eq. (A.4), relating galaxy age and lookback time.

In order to compute the integral in eq. (3.12), we need to measure  $t_{\text{age}}$  as a function of redshift. If measurements below  $z_{\text{min}}$  are lacking, we have to take the integral  $\int_0^{z_{\text{min}}} t_{\text{age}}(x) dx$  into account. Fortunately this constant can be added to  $T$ . The integral  $I$  is therefore related to galaxy ages via

$$I(z) = H_0 \left[ \mathcal{I} - t_{\text{age}}(z)(1+z) + \int_{z_{\text{min}}}^z t_{\text{age}}(x) dx \right], \quad (3.13)$$

where we have defined a new constant

$$\mathcal{I} = T + \int_0^{z_{\text{min}}} t_{\text{age}}(x) dx, \quad (3.14)$$

which has to be determined from data.

In terms of observable quantities, eq. (2.9) can be rewritten as

$$\Omega_K \simeq \frac{10}{I^2} \left\{ \sqrt{1 + \frac{12}{10} \left[ \frac{\exp \left[ \frac{\ln 10}{5} (m - \mathcal{M}) \right]}{(1+z)I} - 1 \right]} - 1 \right\}, \quad (3.15)$$

i.e.,  $\Omega_K = \Omega_K(I, m - \mathcal{M})$ . The uncertainty in a measurement of the curvature using the integral approach is given by

$$\sigma_{\Omega_K} = \sqrt{\left( \frac{\partial \Omega_K}{\partial I} \sigma_I \right)^2 + \left( \frac{\partial \Omega_K}{\partial (m - \mathcal{M})} \sigma_{m - \mathcal{M}} \right)^2}. \quad (3.16)$$

The right panel in figure 2 shows how the sensitivity of  $\Omega_K$  to the variables  $\theta = \{I, m - \mathcal{M}\}$  varies with redshift. The error decreases with redshift and is dominated by the error in  $I(z)$ . Figure 2 shows that for a given error in  $m - \mathcal{M}$ , the uncertainty in  $\Omega_K$  is larger for the integral than for the differential approach.



### 3.4 Differentiation of data

The differential method relies on estimating derivatives of noisy data, SN Ia magnitudes to get  $m'$  and, in the case we do not have  $H(z)$  data, the derivative of galaxy ages to obtain  $E(z)$  (see section 4.2).

Since, in a flat universe,  $m'$  gives a measure of  $H(z)$ , SN Ia data has been used to show how  $H(z)$  increases with redshift. A common way to derive  $m'$  for this purpose is to use the method described in [27] for extracting the expansion history in uncorrelated redshift bins from SN Ia data [e.g., 18, 21, 28]. It turns out that this method is equivalent to the much simpler method of fitting straight lines to the  $m(z)$  data in redshift bins and use the slope of the fitted lines as estimates of the derivative (with corresponding errors). We have checked that fitting higher order polynomials to the data in a given bin does not affect the estimated slope appreciably<sup>1</sup>.

Having  $n_{\text{SN}}$  SNe Ia with magnitude uncertainty  $\sigma_m$  in a redshift bin of width  $\Delta z$  gives an uncertainty in  $m'$  of

$$\sigma_{m'} \simeq \frac{\sigma_m}{0.2886 \Delta z \sqrt{n_{\text{SN}} - 2}} \quad (3.17)$$

$$\simeq 0.031 \left( \frac{n_{\text{SN}}}{500} \right)^{-1/2} \left( \frac{\Delta z}{0.5} \right)^{-1} \left( \frac{\sigma_m}{0.1} \right). \quad (3.18)$$

This can be compared to the error in  $m - \mathcal{M}$  given by

$$\sigma_{m-\mathcal{M}} = \sqrt{\sigma_m^2 + \sigma_{\mathcal{M}}^2}, \quad (3.19)$$

where

$$\sigma_m \simeq 0.0045 \left( \frac{n_{\text{SN}}}{500} \right)^{-1/2} \left( \frac{\sigma_m}{0.1} \right). \quad (3.20)$$

and  $\sigma_{\mathcal{M}}$  is given by an equivalent formula where  $n_{\text{SN}}$  refers to the number of low redshift SNe Ia.

Estimating  $H(z)$  from  $n_{\text{age}}$  galaxy age estimates with fractional uncertainty  $f_{\text{age}}$  in a redshift bin of width  $\Delta z$ , we obtain

$$\frac{\sigma_H}{H} \simeq 0.031(1+z) \left( \frac{n_{\text{age}}}{500} \right)^{-1/2} \left( \frac{\Delta z}{0.5} \right)^{-1} \left( \frac{f_{\text{age}}}{0.1} \right). \quad (3.21)$$

Besides the error in  $H(z)$ , we must also consider the error in the Hubble constant when estimating the error in  $E(z)$ ,

$$\sigma_E = E \sqrt{\left( \frac{\sigma_H}{H} \right)^2 + \left( \frac{\sigma_{H_0}}{H_0} \right)^2}. \quad (3.22)$$

When combining results from different redshift bins, one must take into account the correlations between the bins since any error in  $\mathcal{M}$  and  $H_0$  will cause a systematic shift in the derived value of  $\Omega_K$ .

---

<sup>1</sup>Note that this equivalent to saying that when estimating the differential using a Savitsky-Golay filter of degree  $n$ , the results is insensitive to  $n$ .

### 3.5 Integration of data

Let us assume that we have measured a set of galaxy ages and their redshifts. The following formula can then be used to compute the integral of  $t_{\text{age}}(z)$  numerically

$$F(z_k) \equiv \int_{z_{\min}}^{z_k} t_{\text{age}}(x) dx \simeq \frac{1}{2} \sum_{j=1}^k (t_{\text{age},j} + t_{\text{age},j-1})(z_j - z_{j-1}), \quad (3.23)$$

where  $z_k > z_j$  if  $k > j$  and we assume  $z_0 = z_{\min}$ . Values of  $F(z_k)$  at different redshifts computed using eq. (3.23) are correlated. In appendix B we compute the covariance matrix,  $U_{jk}$ , for a model where the data points are equidistant in redshift, i.e. the number density is constant. We also assume that the errors are the same for all measurements. For the covariance matrix given by eq. (B.2), we find that  $U_{jk} \lesssim U_{kk}$ , i.e., the off diagonal elements are comparable in magnitude to the variance  $\sigma_F^2 \equiv U_{kk}$ . However, when computing  $I(z)$  using eq. (3.13) other sources of error enter

$$\sigma_I = H_0 \sqrt{\left(\frac{I}{H_0}\right)^2 \left(\frac{\sigma_{H_0}}{H_0}\right)^2 + \sigma_{\mathcal{I}}^2 + (1+z)^2 \sigma_{t_{\text{age}}}^2 + \sigma_F^2}, \quad (3.24)$$

where  $\sigma_{\mathcal{I}}$  is the error in  $\mathcal{I}$ . The two last terms depends on  $t_{\text{age}}$  and we should therefore compare the covariance matrix  $U_{jk}$  with the variance  $(1+z)^2 \sigma_{t_{\text{age}}}^2$ . For our model the covariance is inversely proportional to the number density and can therefore be beaten down by statistics. If we approximate the covariance with eq. (B.3),  $U_{jk}$  will be smaller than  $(1+z)^2 \sigma_{t_{\text{age}}}^2$  as long as the constant number density  $\alpha \equiv dn/dz$  is

$$\alpha > \frac{1}{4} \geq \frac{z - z_{\min}}{(1+z)^2}. \quad (3.25)$$

Let us as an example take  $\alpha = 25$  corresponding to  $n_{\text{age}} \simeq 40$  galaxy ages evenly distributed in the redshift interval  $0 \lesssim z \lesssim 1.5$ . In that case  $U_{jk}$  will be smaller than  $(1+z)^2 \sigma_{t_{\text{age}}}^2$  by a factor 100. In the following we will therefore assume that the error in the integral approximation can be neglected.

## 4 Data

### 4.1 Type Ia supernovae

We use the Union2 [29] compilation of SNe Ia, which is an updated version of the Union data set [30]. This data set contains SNe Ia from, e.g., the Supernova Legacy Survey, ESSENCE survey and HST observations. After selection cuts, the data set amounts to 557 SNe Ia, spanning a redshift range of  $0 \lesssim z \lesssim 1.4$ , analysed in a homogeneous fashion using the spectral-template-based fit method SALT2.

### 4.2 Galaxy ages

In passively evolving galaxies the stellar population was formed at high redshift and has since then been evolving without any further episodes of star formation. Massive galaxies located in high density regions of clusters have old stellar populations and are therefore believed to be passively evolving [31–37]. The ages of the passively evolving galaxies can be inferred

from their spectra using synthetic stellar population models [31, 32, 38, 39]. Spectroscopic dating of galaxies have been used for cosmological purposes in, e.g., [26, 40–43].

We use values of  $H(z)$  derived from measured galaxy ages in [43] for the differential approach (though look at the caveats in section 7). For the integral approach we use measurements of galaxy ages from [42].

### 4.3 Other probes of the Hubble parameter

The Hubble parameter,  $H(z)$ , can in principle be measured with other probes than galaxy ages, e.g., the time drift of redshifts [44] and the dipole of the luminosity distance [45].

In [46], a peak along the radial direction of the 2-point correlation function of LRG galaxies, consistent with the expected BAO signal was found. Using the BAO peak position as a standard ruler in the radial direction, enables a direct measurement of  $H(z)$  either at  $z = 0.24$  and  $z = 0.43$  or at  $z = 0.34$ . See, however, also [47, 48] for discussions of the validity of the results.

For the Hubble constant, throughout this paper, we use  $H_0 = 74.2 \pm 3.6 \text{ km s}^{-1} \text{ Mpc}^{-1}$  as derived from the HST distance ladder observations of Cepheid variables, SNe Ia, and masers [49].

## 5 Results

### 5.1 Differential approach

Combining the Union2 SN Ia data set with values of  $H(z)$  derived from galaxy ages in [43] (again, note the caveats in section 7) and HST Hubble constant constraints, gives the result presented in figure 3. We have collected the data in three redshift bins:  $0.1 \leq z < 0.4$ ,  $0.4 \leq z < 0.8$ , and  $z \geq 0.8$ . Data below  $z = 0.1$  are being used to constrain  $\mathcal{M}$ .

The upper panels show  $m - \mathcal{M}$  and  $m'$  as derived from the Union2 data set. The lower left panel shows  $E(z)$  as derived from galaxy ages [43] with the HST value for  $H_0$  [49]. The dotted lines correspond to the theoretical predictions for a flat cosmological constant universe with  $\Omega_M = 0.3$ . In order to put the data points at the same redshift, we have shifted each data point according to the expected shift given a specific cosmology where the curvature is a free parameter and the matter density is held fixed at  $\Omega_M = 0.3$ . Note however that the results are not sensitive to this shifting, nor to the value of  $\Omega_M$  since the shift is performed over a relatively narrow redshift range. In each redshift bin, we perform a  $\chi^2$ -minimisation to find the best-fitting value of  $\Omega_K$ . The combined constraint on  $\Omega_K$  from all bins (taking the correlation between the bins properly into account, see section 3.4) is shown in the lower right panel, giving  $\Omega_K = -0.50^{+0.66}_{-0.41}$  (95% CL).

Adding  $H(z)$  derived from BAO data to the galaxy age data leads to slightly smaller uncertainties on the expansion history  $E(z)$  and thus also the curvature:  $\Omega_K = -0.50^{+0.54}_{-0.36}$  (95% CL), see figure 4.

### 5.2 Integral approach

We use galaxy ages from [42] to estimate the integral  $I(z)$  as a function of redshift. The relative error in  $t_{\text{age}}$  is assumed to be 10% (L. Verde, private communication). Computing  $I(z)$  via eq. (3.13) requires knowledge of  $H_0$  and  $\mathcal{I}$ . The value of  $\mathcal{I}$  depends on the redshift range of the galaxy ages and when the star formation in the passively evolving galaxies halted, it must therefore be inferred from the data themselves. Since  $\mathcal{I}$  has to be determined

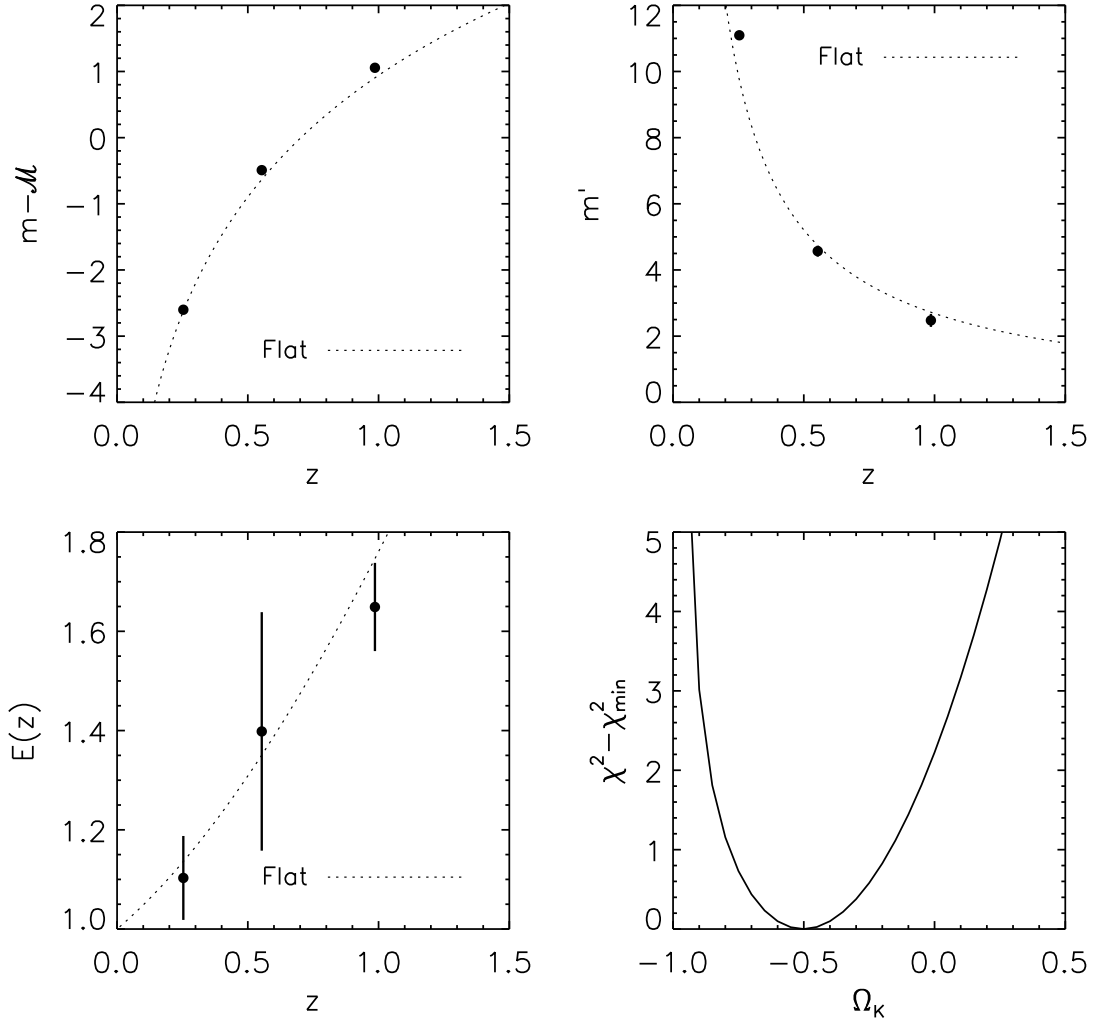


**Figure 3.** *Upper left:*  $m - \mathcal{M}$  for the Union2 data set. Note that the error bars are smaller than the size of the plotting symbols. *Upper right:*  $m'$  for the Union2 data set. *Lower left:* Values of  $E(z)$  derived from galaxy ages in [43] and HST Hubble constant data [49]. The dotted lines correspond to the theoretical predictions for a flat cosmological constant universe with  $\Omega_M = 0.3$ . *Lower right:*  $\chi^2 - \chi^2_{\min}$  as a function of  $\Omega_K$  giving  $\Omega_K = -0.50^{+0.66}_{-0.41}$  (95% CL).

from data, we fit both  $\Omega_K$  and  $\mathcal{I}$  to the data using eq. (2.8) instead of computing  $\Omega_K$  with eq. (3.15). The upper left panel in figure 5 shows  $I(z)$  computed for the best-fitting value of  $\mathcal{I}$  assuming  $H_0 = 74.2 \text{ km s}^{-1} \text{ Mpc}^{-1}$ .

Since SNe Ia and galaxy ages are not measured at the same redshifts, the data are collected in redshift bins of size  $\Delta z = 0.05$ . For the SNe Ia, we require at least 3 SNe per bin when computing the average magnitude,  $\langle m \rangle$ . In bins with more than one value of  $t_{\text{age}}$  we use the average  $\langle (1+z)t_{\text{age}} - F(z) \rangle$ . The binning procedure results in  $n_{\text{bin}} = 11$  bins ranging from  $z_{\text{bin}} = 0.13$  to 1.38. The upper right panel in figure 5 shows the binned values of  $m - \mathcal{M}$ .

Results are also sensitive to the Hubble constant. We therefore include  $H_0$  in the fit

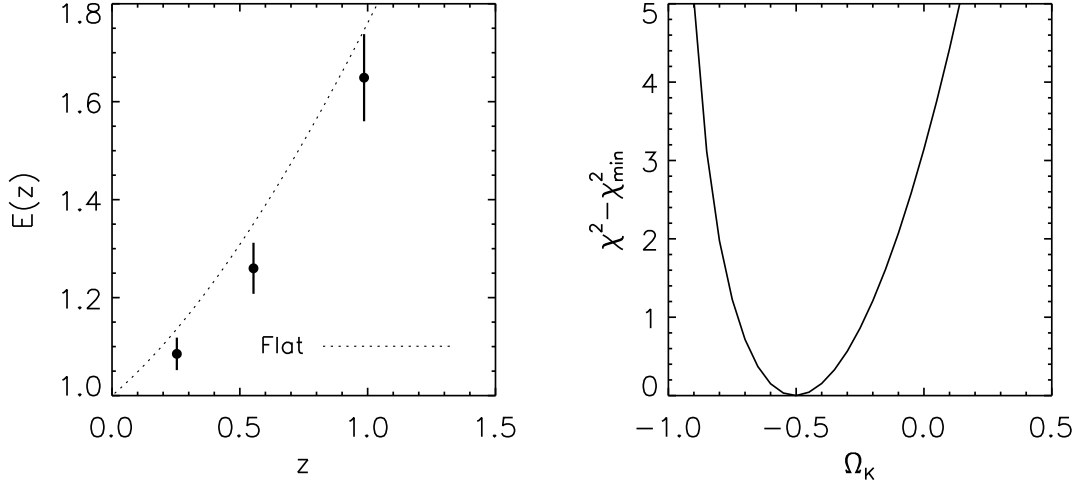


**Figure 4.** *Left:* Values of  $E(z)$  derived from galaxy ages in [43], radial BAO constraints from [46], and HST Hubble constant data [49]. The dotted line corresponds to the theoretical prediction for a flat cosmological constant universe with  $\Omega_M = 0.3$ . *Right:*  $\chi^2 - \chi_{\min}^2$  as a function of  $\Omega_K$  giving  $\Omega_K = -0.50^{+0.54}_{-0.36}$  (95% CL).

and then marginalise over it assuming a Gaussian prior to obtain constraints on  $\Omega_K$  and  $\mathcal{I}$ . Using the binned data, we fit  $\Omega_K$ ,  $\mathcal{I}$ , and  $H_0$  to the data using the following  $\chi^2$ -statistic

$$\chi^2 = \sum_{j=1}^{n_{\text{bin}}} \frac{\left[ D_j - \left( I_j + \frac{\Omega_K}{6} I_j^3 + \frac{\Omega_K^2}{120} I_j^5 \right) \right]^2}{\sigma_{D_j}^2 + \left( 1 + \frac{\Omega_K}{2} I_j^2 + \frac{\Omega_K^2}{24} I_j^4 \right)^2 \sigma_{I_j}^2}, \quad (5.1)$$

where  $D_j = (1 + z_{\text{bin},j})^{-1} \exp \left[ \frac{\ln 10}{5} (\langle m \rangle_j - \mathcal{M}) \right]$  and  $I_j = H_0 [\mathcal{I} - \langle (1+z)t_{\text{age}} + F(z) \rangle_j]$ . The errors  $\sigma_{D_j}$  and  $\sigma_{I_j}$  are computed using error propagation from the measurements uncertainties in SN Ia magnitudes and galaxy ages, respectively.

The lower left panel in figure 5 shows the confidence levels in the  $[\Omega_K, \mathcal{I}]$ -plane at 68.3 and 95% CL. These constraints were obtained after marginalisation over the Hubble constant using the results of Riess et al. [49] as a Gaussian prior. Again we use a fixed value of  $\mathcal{M}$  determined from low redshift SNe Ia.

The lower right panel in figure 5 shows  $\chi^2 - \chi_{\min}^2$  as a function of  $\Omega_K$  after marginalisation over  $\mathcal{I}$ . Our constraints on the curvature is  $\Omega_K = 0.29^{+1.65}_{-0.94}$  (95% CL).

## 6 Future

Current data clearly give quite weak constraints on  $\Omega_K$ . In this section, we investigate the possibility to constrain the spatial curvature using future distance and age, or  $H(z)$ , data. As our default future data set, we assume that we will have 2000 well observed SNe Ia in the range  $0.002 \leq z \leq 1.5$  with  $\sigma_m = 0.1$  mag. For passive galaxy ages, we assume 2000 measurements in the range  $0.1 \leq z \leq 1.5$  with a precision of 0.1 Gyr. Since these numbers are subject to large uncertainties, we also discuss how our results scale with the total number

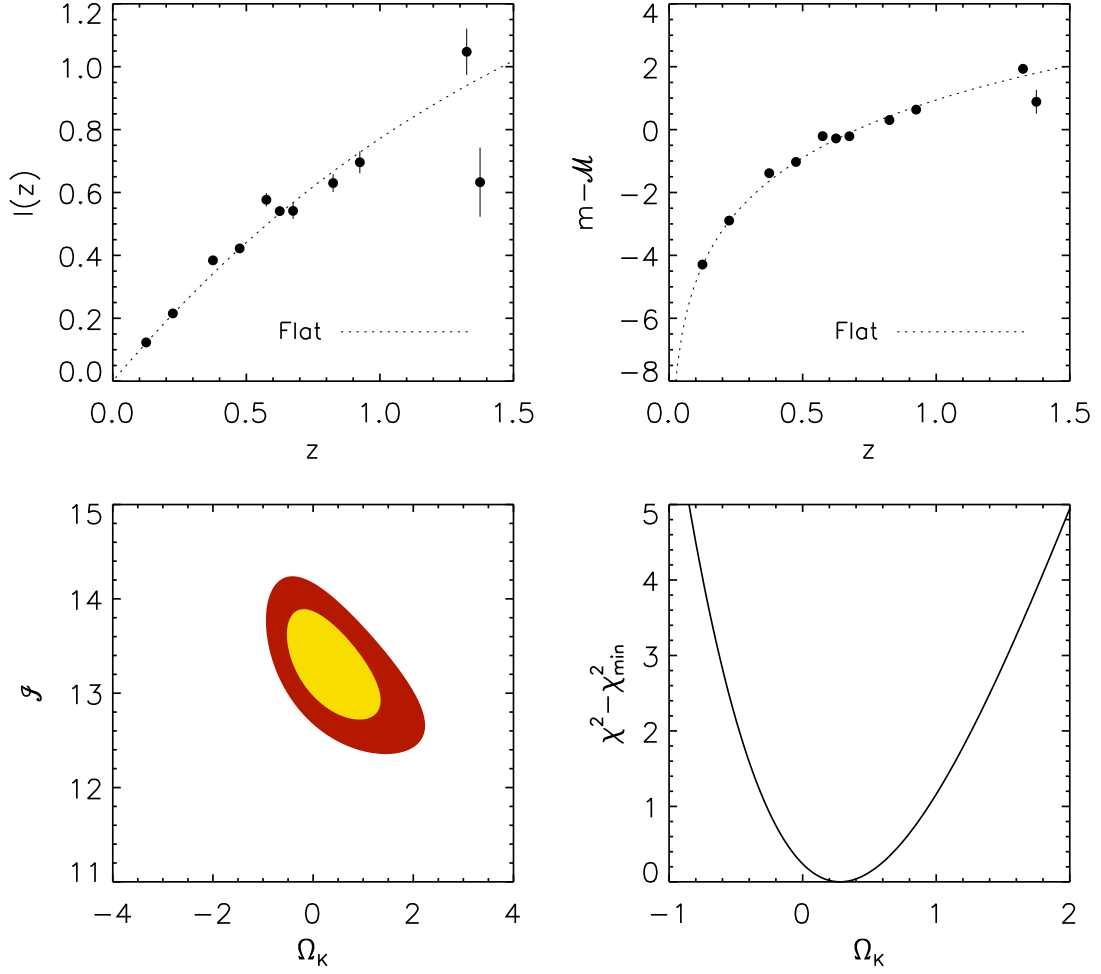


**Figure 5.** *Upper left:*  $I(z)$  derived in redshift bins using galaxy ages from [42]. The best-fitting value of  $\mathcal{I}$  and  $H_0 = 74.2 \text{ km s}^{-1} \text{ Mpc}^{-1}$  were used to compute  $I(z)$  using eq. (3.13). *Upper right:*  $m - \mathcal{M}$  for the same redshift bins computed using the Union2 data [29] and a value of  $\mathcal{M}$  fitted to low redshift data. *Lower left:* Confidence contours in the  $[\Omega_K, \mathcal{I}]$ -plane at the 68.3 and 95% CL after marginalisation over  $H_0$  assuming a Gaussian prior. *Lower right:*  $\chi^2 - \chi_{\min}^2$  as a function of  $\Omega_K$  giving  $\Omega_K = 0.29^{+1.65}_{-0.94}$  (95% CL).

and redshift distribution of the data. If not otherwise stated, we assume that  $H_0$  has an uncertainty of one percent. Our fiducial cosmology is a flat universe with  $\Omega_M = 0.3$  and  $\Omega_\Lambda = 0.7$ .

### 6.1 Differential approach

For our default future data set, the differential method gives the results depicted in figure 6, where we have  $\Omega_K = 0.003 \pm 0.23$  (95% CL). In addition, we have assumed that we have on the order of 1000 SNe Ia at low redshifts in order to calibrate  $\mathcal{M}$ , although the error contribution would be negligible also for a much smaller number of low redshift SNe.

This error on  $\Omega_K$  is comparable to what one can get with future percent level bounds on the expansion rate, e.g. from radial BAO measurements, instead of the galaxy ages. In

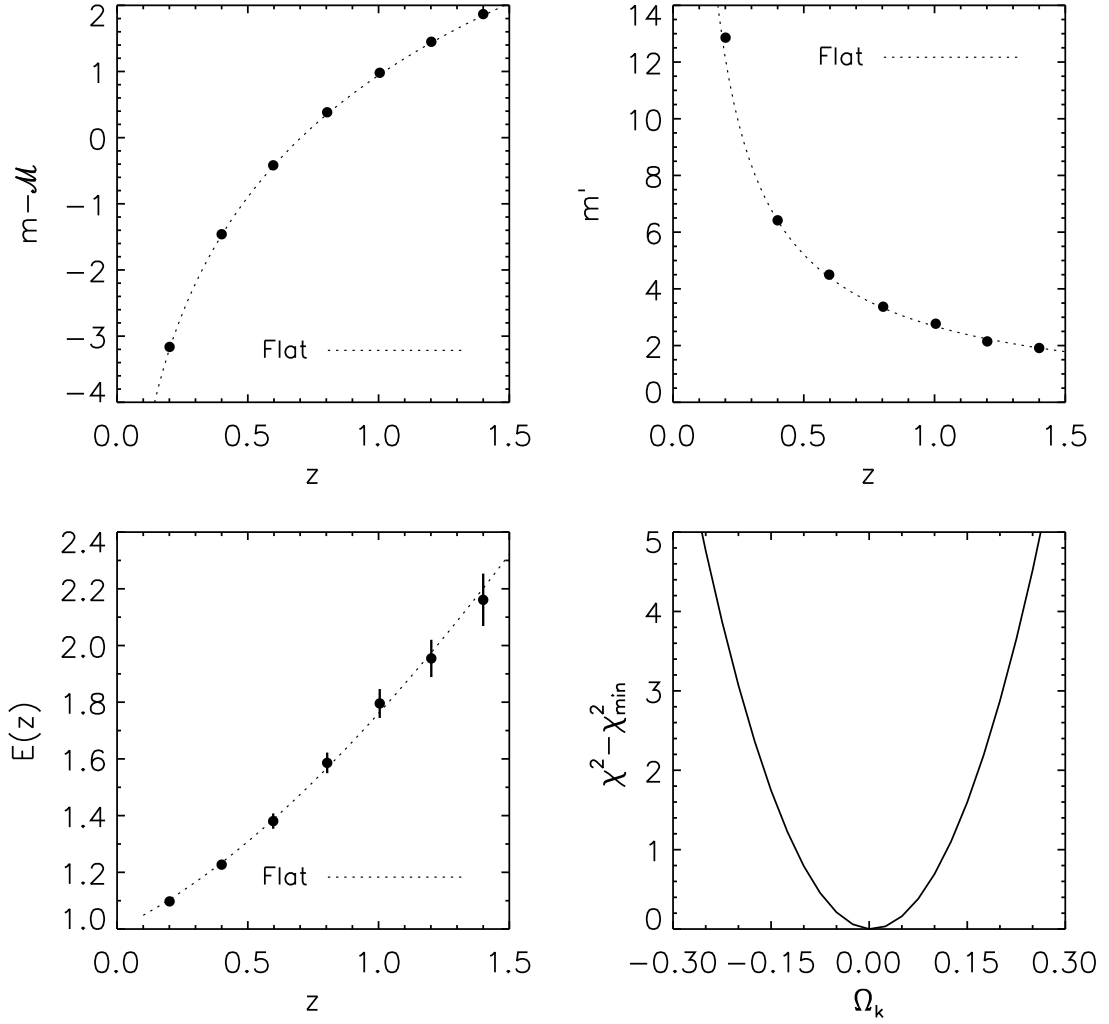


**Figure 6.** Future constraints on  $\Omega_K$  with 2000 well observed SNe Ia in the range  $0.002 \leq z \leq 1.5$  with  $\sigma_m = 0.1$  mag and 2000 galaxy age measurements in the range  $0.1 \leq z \leq 1.5$  with a precision of 0.1 Gyr. *Upper left:*  $m - \mathcal{M}$  as derived from SN Ia distances. *Upper right:*  $m'$  as derived from SN Ia distances. *Lower left:*  $E(z)$  derived from galaxy ages. The dotted lines are for a flat cosmology with  $\Omega_M = 0.3$  and a cosmological constant. *Lower right:* The resulting  $\chi^2 - \chi^2_{\min}$  giving  $\Omega_K = 0.003 \pm 0.23$  (95% CL).

[50], it is shown that a future large high-redshift spectroscopic galaxy survey covering 10 000 square degrees could give a measure of  $H(z)$  at the few percent level in redshift bins of size  $\Delta z = 0.2$  in the redshift interval  $0.5 < z < 1.5$  by measuring the radial BAO signal. Combining these data with our default SN Ia data set, we typically obtain results as depicted in figure 7, where we have  $\Omega_K = 0.04 \pm 0.22$  (95% CL).

We note that our error scales as the inverse of the square root of the number of SNe and/or galaxy ages, depending on which dominates the error budget. For our default data set, the error contribution from  $E(z)$  and  $m'$  are comparable at low redshifts whereas at high redshifts, errors from  $m'$  dominate. Generally, the errors from  $m - \mathcal{M}$  are negligible.

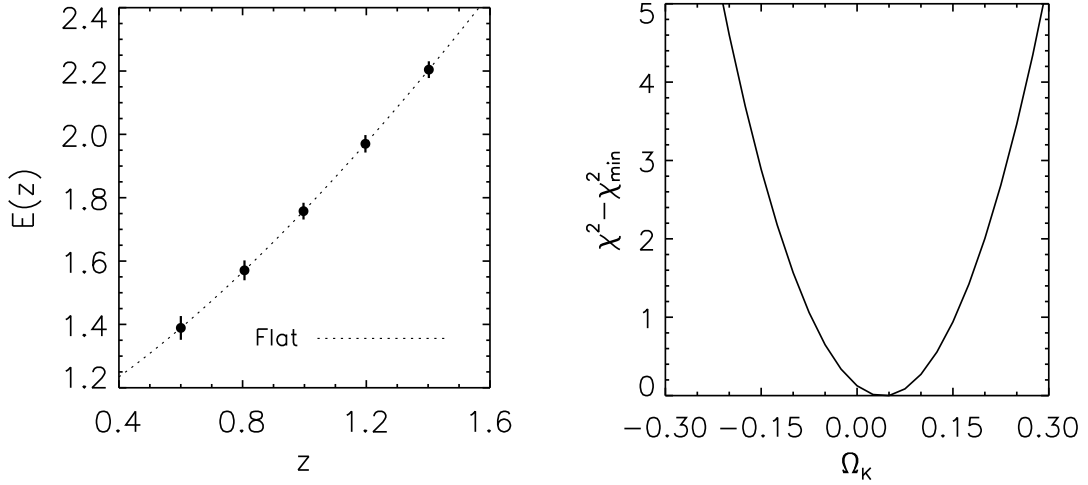


**Figure 7.** Future constraints on  $\Omega_K$  with 2000 well observed SNe Ia in the range  $0.002 \leq z \leq 1.5$  with  $\sigma_m = 0.1$  mag and constraints on  $H(z)$  at the few percent level in redshift bins of size  $\Delta z = 0.2$  in the redshift interval  $0.5 < z < 1.5$  from future galaxy surveys [50]. *Left:*  $E(z)$  as derived from the radial BAO signal in future galaxy surveys and Hubble constant constraints. The dotted line is for a flat cosmology with  $\Omega_M = 0.3$  and a cosmological constant. *Lower right:* The resulting  $\chi^2 - \chi_{\min}^2$  giving  $\Omega_K = 0.04 \pm 0.22$  (95% CL).

## 6.2 Integral approach

Applying the integral approach to our default future data set, we obtain the result depicted in figure 8. After marginalisation over  $\mathcal{I}$ , we find  $\Omega_K = -0.005 \pm 0.054$  (95% CL). Here we have assumed perfect knowledge of  $\mathcal{M}$  and a 1% prior on  $H_0$ . In table 1, we show constraints at the 95% CL for different values of  $n_{\text{sn}}$  and  $n_{\text{age}}$ . From this table we learn two things: First, increasing only one of the number helps, but is not as effective as increasing both, i.e., for the numbers used, neither the errors from SNe or galaxy ages dominate completely the error budget. Consequently,  $n_{\text{sn}} = n_{\text{age}}$  is optimal. From an observational point of view it might however be easier and less expensive to increase one of the two numbers. Second, for  $n_{\text{sn}} = n_{\text{age}}$ , the errors scale as  $n^{-1/2}$ . This implies that reaching an error in  $\Omega_K$  of  $\simeq 0.01$  at the 95% CL requires  $n_{\text{sn}} = n_{\text{age}} \simeq 5 \cdot 10^4$ .

We have also investigated the sensitivity of our results with respect to the Hubble constant prior in the case where  $n_{\text{SN}} = n_{\text{age}} = 500$ . If the value of  $H_0$  was perfectly known, we would anticipate a measurement with an uncertainty of 0.052 at the 95% CL. Assuming a 1% Gaussian prior increases this number to 0.098. Increasing the prior to 2% and 5% results in 0.110 and 0.119, respectively. Our forecast are clearly not too dependent on our choice of the  $H_0$  prior.

The redshift range of the data is important. The higher the redshift, the more constraining power our method have. Assuming  $n_{\text{SN}} = n_{\text{age}} = 500$  but data distributed in the interval  $0.002 \leq z \leq 1.0$  we find the uncertainty in  $\Omega_K$  to be 0.173 at the 95% CL. Keeping the number of data points fixed and increasing the maximum redshift to 2 and 2.5 leads to an uncertainty in  $\Omega_K$  of 0.065 and 0.054 at the 95% CL, respectively.



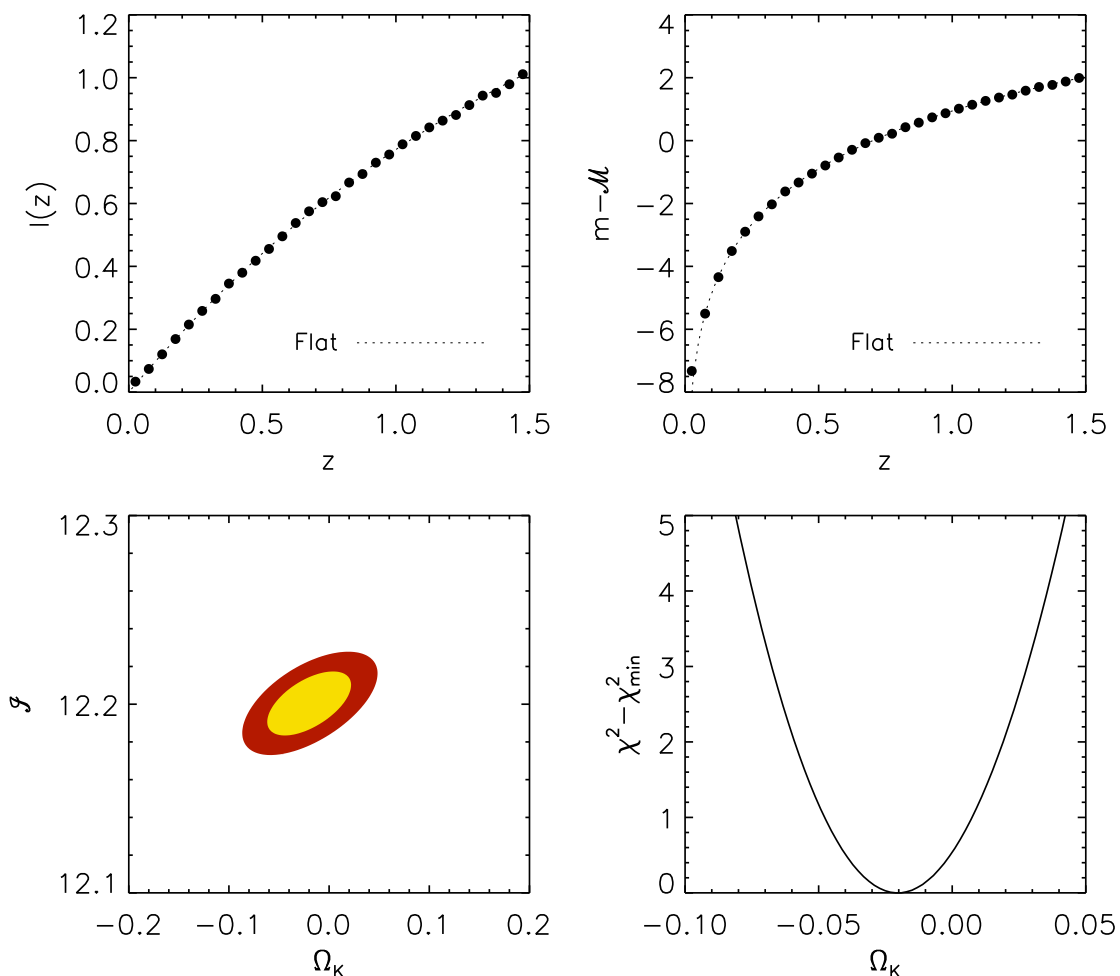


**Figure 8.** Future constraints on  $\Omega_K$  with 2000 well observed SNe Ia in the range  $0.002 \leq z \leq 1.5$  with  $\sigma_m = 0.1$  mag and 2000 galaxy age measurements in the range  $0.1 \leq z \leq 1.5$  with a precision of 0.1 Gyr. *Upper left:*  $I(z)$  as derived from galaxy ages. *Upper right:*  $m - \mathcal{M}$  as derived from SN Ia distances. *Lower left:* Confidence contours in the  $[\Omega_K, \mathcal{I}]$ -plane at the 68.3% and 95% CL after marginalisation over  $H_0$  assuming a 1% Gaussian prior. *Lower right:* The resulting  $\chi^2 - \chi^2_{\min}$  giving  $\Omega_K = -0.005 \pm 0.054$  (95% CL).

## 7 Summary and Discussion

We have investigated how the large scale spatial curvature of the Universe can be measured model independently. Cosmological distances depend on  $\Omega_K$  via the expansion history and the geometrical path of photons. If the two contributions can be disentangled,  $\Omega_K$  can be measured independently of the energy content of the Universe. We have pursued two different paths to disentangle the effects of geometry and expansion.

The *differential* approach, originally suggested by Clarkson, Cort  s, and Basset [6], allows  $\Omega_K$  to be measured via eq. (2.7). In addition to distances, this approach requires derivatives of distance with respect to redshift and independent measurements of the expansion history. The expansion history can be measured using different probes. Here we

**Table 1.** Constraints on  $\Omega_K$  at the 95% CL from simulated SN Ia and galaxy age data. The data is uniformly distributed in the redshift interval  $0.002 < z < 1.5$ . For SNe Ia and galaxy ages the error is  $\sigma_m = 0.1$  mag and  $\sigma_{t_{\text{age}}} = 0.1$  Gyr, respectively. The value of the Hubble constant was assumed to be known to 1%.

$n_{\text{SN}}$	$n_{\text{age}} = 100$	$n_{\text{age}} = 500$	$n_{\text{age}} = 1000$	$n_{\text{age}} = 2000$
100	0.188	0.188	0.165	0.156
500	0.122	0.098	0.093	0.084
1000	0.111	0.080	0.072	0.066
2000	0.104	0.069	0.060	0.054

focus on the method proposed by Jimenez and Loeb [26], which utilises relative galaxy ages. Cosmological distances with corresponding redshift derivatives can be derived from SN Ia observations.

The differential approach requires numerical derivation of data to obtain  $D'(z)$ , and in the case of galaxy ages, also  $E(z)$ . Numerical derivation of noisy data is far from trivial and we suspect that errors have often been underestimated in the past. In [42], for example, they use a customised method to obtain  $H(z)$  that gives uncomfortably small errors. Basically, they first group together all galaxies that are within  $\Delta z = 0.03$  of each other to get an estimate of the age of the universe at a given redshift with as many galaxies as possible. The redshift interval is chosen to be small enough to avoid incorporating galaxies that have already evolved in age, but large enough to have more than one galaxy in most of the bins. Age differences are computed only for those bins in redshift that are separated by more than  $z = 0.1$  but not by more than  $z = 0.15$ . The first limit is imposed so that the age evolution between the two bins is larger than the error in the age determination. The authors claim that this procedure provides a robust determination of  $dz/dt_{\text{age}}$ . We have not been able to reproduce their results and have therefore not been able to check the stability of this claim. It is, however, unlikely that the given uncertainties in the derived values of  $H(z)$  are correct. From a sample of 32 galaxy ages (out of which some are discarded as outliers), you could form a maximum of 16 pairs of 2 galaxy ages each which could give 8 values of the Hubble parameter. Assuming an error of 10% in the galaxy ages, a simple analytical error propagation gives an error of  $\gtrsim 100\%$  in  $H(z)$ . A straight line fit in bins give similar results; at best a 100% error on  $H(z)$  at five different redshifts. With this (lack of) precision it turns out to be futile to determine  $\Omega_K$ . In [43],  $dt_{\text{age}}/dz$  is computed by defining the edge in the  $t_{\text{age}}$  vs  $z$ -plot formed by the oldest galaxies in a sample of 24 clusters, yielding two additional  $H(z)$  estimates at  $z = 0.48$  and  $0.9$ . We have not checked the stability of this method but the derived  $H(z)$  uncertainties seems to be more reasonable when compared to the number of galaxy ages employed.

Galaxy ages as a function of redshift can, alternatively, be used to measure the integral  $I(z)$  via eq. (3.13). Knowledge of  $I(z)$  allows  $\Omega_K$  to be measured via the *integral* approach, see eq. (2.9). This approach requires numerical integration of noisy data instead of numerical differentiation. There are potential problems also with the integral method. The integral approach, which relies on measurements of lookback time, is not as general as the differential approach, where, in principle,  $E(z)$  can be measured using several fundamentally different methods. We assume that the lookback time can be measured via passively evolving galaxies acting as cosmic chronometers. When converting galaxy ages to lookback times we make the

assumption that the star formation halted at the same time, i.e., that all passively evolving galaxies share the same birthday. Even if a population of cosmic chronometers exists, there is always a risk that our sample is contaminated by other galaxies. Two unknown quantities enter our calculation of  $I(z)$ : the constant offset in time between galaxy age and lookback time and the low redshift part of the integral over galaxy age. Fortunately, these unknowns can be handled by a single nuisance parameter  $\mathcal{I}$ . The need for an extra nuisance parameter is however another drawback of the method as it degrades the constraining power of the data. Another problem with the integral method is that values of  $I(z)$  computed using eq. (3.23) are correlated. However, as shown in appendix B the correlations decrease with increasing number of galaxy ages.

Generally, the differential method is the most effective if we have, in addition to distance measures, independent  $H(z)$  constraints from, e.g., radial BAO measurements. The integral method, on the other hand, outperforms the differential method if the expansion history needs to be reconstructed from lookback time measurements. The reason why this is not the case for current data is that the derived  $H(z)$  from passive galaxy ages probably have underestimated uncertainties.

The model independent constraints on  $\Omega_K$  we present here are rather weak,  $-1 \lesssim \Omega_K \lesssim 1$  at the 95% CL, and at least for the differential method, there are reasonable doubts that the uncertainty in the derived expansion history has been underestimated. We therefore investigated to what degree a proper analysis of future data could sharpen current curvature constraints. Even if the amount of data is significantly increased, we find that the uncertainty in  $\Omega_K$  will be fairly large,  $\simeq 0.1$  at the 95% CL, at least compared to (model dependent) CMB constraints. It is therefore unrealistic that the methods presented in this paper will be able to constrain, e.g. inflationary models that predict spatial curvature on the order of  $|\Omega_K| \lesssim 10^{-5}$ .

In the introduction we noted another proposed method of measuring  $\Omega_K$  model independently using weak gravitational lensing and BAO by Bernstein [20]. Forecasts for this method, assuming a full sky survey of galaxies in the redshift range  $0 < z < 3$  supplemented with photometric redshifts, predicts an uncertainty in  $\Omega_K$  of  $\simeq 0.04$  at the 68.3% CL. This precision is comparable to what could be obtained with the integral method with  $n_{sn} = 1000$  and  $n_{age} = 500$  (see table 1).

## Acknowledgments

EM acknowledge support for this study by the Swedish Research Council. We thank Licia Verde for kindly providing us with galaxy ages in electronic form. JJ would like to thank Rahman Amanullah for fruitful discussions.

## A Lookback time and galaxy ages

The integral  $I(z)$  can, according to eq. (3.12), be obtained from measurements of lookback time as function of redshift. We assume that the lookback time can be measured via the age of galaxies, or rather the age of the stellar population in galaxies.

To understand the relationship between lookback time and galaxy age, we write the present age of the Universe as

$$t_0 - t_\infty = - \int_0^\infty \frac{dt}{dz} dz \quad (\text{A.1})$$

$$= (t_0 - t_z) + (t_z - t_c) + (t_c - t_\infty), \quad (\text{A.2})$$

where  $t_0 - t_z$  is the lookback time,  $t_z - t_c$  is the age of a galaxy at redshift  $z$ , which was created at redshift  $z_c$ , and  $t_c - t_\infty$  is the age of the Universe when the passively evolving stellar population of the galaxy was created.

We naively assume that all the galaxies share a common time of star formation. In that case

$$(t_0 - t_z) = T - (t_z - t_c), \quad (\text{A.3})$$

where the constant  $T$  is the age of the Universe at redshift  $z_c$  subtracted from the present age of the Universe. The lookback time and the galaxy age are hence related by an additive constant. Consequently galaxy ages are related to  $\tau$  through

$$\tau = H_0(T - t_{\text{age}}). \quad (\text{A.4})$$

## B Derivation of error in the integral approximation

We use eq. (3.23) to compute the area under the graph of  $t_{\text{age}}(z)$ . Let us make some simplifying assumptions that will allow us to draw some conclusions about the accuracy of the approximation. We assume all the measurements  $t_{\text{age},i}$  at redshifts  $z_i$  to be separated by  $\Delta z$ . Furthermore we assume the error  $\sigma_{t_{\text{age}}}$  to be the same for all  $t_{\text{age},i}$ . Values of  $F(z)$  computed at different redshifts using eq. (3.23) are obviously correlated. With the previous assumptions, we can derive an approximate formula for the covariance matrix using error propagation,

$$U_{jk} \simeq \sum_{i=0}^{\min(j,k)} \frac{\partial F_j}{\partial t_{\text{age},i}} \frac{\partial F_k}{\partial t_{\text{age},i}} \sigma_{t_{\text{age}}}^2 = \left[ \min(j,k) - \frac{1}{4}(1 + \delta_{jk}) \right] \Delta z^2 \sigma_{t_{\text{age}}}^2 \lesssim \min(j,k) \Delta z^2 \sigma_{t_{\text{age}}}^2. \quad (\text{B.1})$$

The assumption that the points are evenly distributed in redshift means that  $dn/dz = \alpha$  is a constant. Consequently  $k = \alpha(z_k - z_{\min})$  and  $\Delta z = \alpha^{-1}$ . We can therefore rewrite the covariance in terms of redshift as

$$U_{jk} \lesssim \frac{\sigma_{t_{\text{age}}}^2}{\alpha} [\min(z_j, z_k) - z_{\min}]. \quad (\text{B.2})$$

At redshift  $z_k$  the variance is hence

$$\sigma_F^2 \equiv U_{kk} \lesssim \frac{\sigma_{t_{\text{age}}}^2}{\alpha} (z_k - z_{\min}). \quad (\text{B.3})$$

We note that  $U_{jk} \lesssim U_{kk}$ .

## References

- [1] E. Komatsu, J. Dunkley, M. R. Nolta, C. L. Bennett, B. Gold, G. Hinshaw, N. Jarosik, D. Larson, M. Limon, L. Page, D. N. Spergel, M. Halpern, R. S. Hill, A. Kogut, S. S. Meyer, G. S. Tucker, J. L. Weiland, E. Wollack, and E. L. Wright, *Five-Year Wilkinson Microwave Anisotropy Probe Observations: Cosmological Interpretation*, *Astrophys. J. S.* **180** (2009) 330, [[arXiv:0803.0547](#)].
- [2] R. Kessler, A. C. Becker, D. Cinabro, J. Vanderplas, J. A. Frieman, J. Marriner, T. M. Davis, B. Dilday, J. Holtzman, S. W. Jha, H. Lampeitl, M. Sako, M. Smith, C. Zheng, R. C. Nichol, B. Bassett, R. Bender, D. L. Depoy, M. Doi, E. Elson, A. V. Filippenko, R. J. Foley, P. M. Garnavich, U. Hopp, Y. Ihara, W. Ketzeback, W. Kollatschny, K. Konishi, J. L. Marshall, R. J. McMillan, G. Miknaitis, T. Morokuma, E. Mörtzell, K. Pan, J. L. Prieto, M. W. Richmond, A. G. Riess, R. Romani, D. P. Schneider, J. Sollerman, N. Takanashi, K. Tokita, K. van der Heyden, J. C. Wheeler, N. Yasuda, and D. York, *First-Year Sloan Digital Sky Survey-II Supernova Results: Hubble Diagram and Cosmological Parameters*, *Astrophys. J. S.* **185** (2009) 32, [[arXiv:0908.4274](#)].
- [3] L. Knox, *Precision measurement of the mean curvature*, *Physical Review D* **73** (2006), no. 2 023503.
- [4] J. L. Crooks, J. O. Dunn, P. H. Frampton, H. R. Norton, and T. Takahashi, *Cosmic degeneracy with dark energy equation of state*, *Astroparticle Physics* **20** (2003) 361.
- [5] D. Polarski and A. Ranquet, *On the equation of state of dark energy*, *Physics Letters B* **627** (2005) 1.
- [6] C. Clarkson, M. Cortês, and B. Bassett, *Dynamical dark energy or simply cosmic curvature?*, *Journal of Cosmology and Astro-Particle Physics* **8** (2007) 11.
- [7] Z. Huang, B. Wang, and R. Su, *Uncertainty on Determining the Dark Energy Equation of State due to the Spatial Curvature*, *International Journal of Modern Physics A* **22** (2007) 1819.
- [8] G. Barenboim, E. Fernández Martínez, O. Mena, and L. Verde, *The dark side of curvature*, *Journal of Cosmology and Astro-Particle Physics* **3** (2010) 8, [[arXiv:0910.0252](#)].
- [9] Y. Gong and Y. Zhang, *Probing the curvature and dark energy*, *Physical Review D* **72** (2005) 043518.
- [10] K. Ichikawa and T. Takahashi, *Dark energy evolution and the curvature of the universe from recent observations*, *Physical Review D* **73** (2006) 083526.
- [11] K. Ichikawa, M. Kawasaki, T. Sekiguchi, and T. Takahashi, *Implications of dark energy parametrizations for the determination of the curvature of the universe*, *Journal of Cosmology and Astro-Particle Physics* **12** (2006) 5.
- [12] E. L. Wright, *Constraints on Dark Energy from Supernovae, Gamma-Ray Bursts, Acoustic Oscillations, Nucleosynthesis, Large-Scale Structure, and the Hubble Constant*, *Astrophys. J.* **664** (2007) 633.
- [13] G. Zhao, J. Xia, H. Li, C. Tao, J. Virey, Z. Zhu, and X. Zhang, *Probing for dynamics of dark energy and curvature of universe with latest cosmological observations*, *Physics Letters B* **648** (2007) 8.
- [14] B. A. Reid, W. J. Percival, D. J. Eisenstein, L. Verde, D. N. Spergel, R. A. Skibba, N. A. Bahcall, T. Budavari, J. A. Frieman, M. Fukugita, J. R. Gott, J. E. Gunn, Ž. Ivezić, G. R. Knapp, R. G. Kron, R. H. Lupton, T. A. McKay, A. Meiksin, R. C. Nichol, A. C. Pope, D. J. Schlegel, D. P. Schneider, C. Stoughton, M. A. Strauss, A. S. Szalay, M. Tegmark, M. S. Vogeley, D. H. Weinberg, D. G. York, and I. Zehavi, *Cosmological constraints from the clustering of the Sloan Digital Sky Survey DR7 luminous red galaxies*, *MNRAS* **404** (2010) 60, [[arXiv:0907.1659](#)].

- [15] A. Vikhlinin, A. V. Kravtsov, R. A. Burenin, H. Ebeling, W. R. Forman, A. Hornstrup, C. Jones, S. S. Murray, D. Nagai, H. Quintana, and A. Voevodkin, *Chandra Cluster Cosmology Project III: Cosmological Parameter Constraints*, *Astrophys. J.* **692** (2009) 1060, [[arXiv:0812.2720](#)].
- [16] E. Komatsu, K. M. Smith, J. Dunkley, C. L. Bennett, B. Gold, G. Hinshaw, N. Jarosik, D. Larson, M. R. Nolte, L. Page, D. N. Spergel, M. Halpern, R. S. Hill, A. Kogut, M. Limon, S. S. Meyer, N. Odegard, G. S. Tucker, J. L. Weiland, E. Wollack, and E. L. Wright, *Seven-year Wilkinson Microwave Anisotropy Probe (WMAP) Observations: Cosmological Interpretation*, *Astrophys. J. S.* **192** (2011) 18, [[arXiv:1001.4538](#)].
- [17] K. Ichikawa and T. Takahashi, *Dark energy parametrizations and the curvature of the universe*, *Journal of Cosmology and Astro-Particle Physics* **2** (2007) 1.
- [18] E. Mörtzell and C. Clarkson, *Model independent constraints on the cosmological expansion rate*, *Journal of Cosmology and Astro-Particle Physics* **1** (2009) 44, [[arXiv:0811.0981](#)].
- [19] M. J. Mortonson, *Testing flatness of the universe with probes of cosmic distances and growth*, *Physical Review D* **80** (2009) 123504, [[arXiv:0908.0346](#)].
- [20] G. Bernstein, *Metric Tests for Curvature from Weak Lensing and Baryon Acoustic Oscillations*, *Astrophys. J.* **637** (2006) 598.
- [21] J. Sollerman, E. Mörtzell, T. M. Davis, M. Blomqvist, B. Bassett, A. C. Becker, D. Cinabro, A. V. Filippenko, R. J. Foley, J. Frieman, P. Garnavich, H. Lampeitl, J. Marriner, R. Miquel, R. C. Nichol, M. W. Richmond, M. Sako, D. P. Schneider, M. Smith, J. T. Vanderplas, and J. C. Wheeler, *First-Year Sloan Digital Sky Survey-II (SDSS-II) Supernova Results: Constraints on Nonstandard Cosmological Models*, *Astrophys. J.* **703** (2009) 1374, [[arXiv:0908.4276](#)].
- [22] M. Blomqvist and E. Mörtzell, *Supernovae as seen by off-center observers in a local void*, *Journal of Cosmology and Astro-Particle Physics* **5** (2010) 6, [[arXiv:0909.4723](#)].
- [23] M. Blomqvist, E. Mörtzell, and S. Nobili, *Probing dark energy inhomogeneities with supernovae*, *Journal of Cosmology and Astro-Particle Physics* **6** (2008) 27, [[arXiv:0806.0496](#)].
- [24] C. Clarkson, B. Bassett, and T. Lu, *A General Test of the Copernican Principle*, *Physical Review L* **101** (2008) 011301, [[arXiv:0712.3457](#)].
- [25] A. Shafieloo and C. Clarkson, *Model independent tests of the standard cosmological model*, *Physical Review D* **81** (2010), no. 8 083537, [[arXiv:0911.4858](#)].
- [26] R. Jimenez and A. Loeb, *Constraining Cosmological Parameters Based on Relative Galaxy Ages*, *Astrophys. J.* **573** (2002) 37.
- [27] Y. Wang and M. Tegmark, *Uncorrelated measurements of the cosmic expansion history and dark energy from supernovae*, *Physical Review D* **71** (2005), no. 10 103513.
- [28] A. G. Riess, L. Strolger, S. Casertano, H. C. Ferguson, B. Mobasher, B. Gold, P. J. Challis, A. V. Filippenko, S. Jha, W. Li, J. Tonry, R. Foley, R. P. Kirshner, M. Dickinson, E. MacDonald, D. Eisenstein, M. Livio, J. Younger, C. Xu, T. Dahlsen, and D. Stern, *New Hubble Space Telescope Discoveries of Type Ia Supernovae at  $z \geq 1$ : Narrowing Constraints on the Early Behavior of Dark Energy*, *Astrophys. J.* **659** (2007) 98.
- [29] R. Amanullah, C. Lidman, D. Rubin, G. Aldering, P. Astier, K. Barbary, M. S. Burns, A. Conley, K. S. Dawson, S. E. Deustua, M. Doi, S. Fabbro, L. Faccioli, H. K. Fakhouri, G. Folatelli, A. S. Fruchter, H. Furusawa, G. Garavini, G. Goldhaber, A. Goobar, D. E. Groom, I. Hook, D. A. Howell, N. Kashikawa, A. G. Kim, R. A. Knop, M. Kowalski, E. Linder, J. Meyers, T. Morokuma, S. Nobili, J. Nordin, P. E. Nugent, L. Östman, R. Pain, N. Panagia, S. Perlmutter, J. Raux, P. Ruiz-Lapuente, A. L. Spadafora, M. Strovink, N. Suzuki, L. Wang, W. M. Wood-Vasey, N. Yasuda, and T. Supernova Cosmology Project, *Spectra and Hubble*



*Space Telescope Light Curves of Six Type Ia Supernovae at  $0.511 < z < 1.12$  and the Union2 Compilation*, *Astrophys. J.* **716** (2010) 712, [[arXiv:1004.1711](#)].

- [30] M. Kowalski, D. Rubin, G. Aldering, R. J. Agostinho, A. Amadon, R. Amanullah, C. Balland, K. Barbary, G. Blanc, P. J. Challis, A. Conley, N. V. Connolly, R. Covarrubias, K. S. Dawson, S. E. Deustua, R. Ellis, S. Fabbro, V. Fadeyev, X. Fan, B. Farris, G. Folatelli, B. L. Frye, G. Garavini, E. L. Gates, L. Germany, G. Goldhaber, B. Goldman, A. Goobar, D. E. Groom, J. Haissinski, D. Hardin, I. Hook, S. Kent, A. G. Kim, R. A. Knop, C. Lidman, E. V. Linder, J. Mendez, J. Meyers, G. J. Miller, M. Moniez, A. M. Mourao, H. Newberg, S. Nobili, P. E. Nugent, R. Pain, O. Perdureau, S. Perlmutter, M. M. Phillips, V. Prasad, R. Quimby, N. Regnault, J. Rich, E. P. Rubenstein, P. Ruiz-Lapuente, F. D. Santos, B. E. Schaefer, R. A. Schommer, R. C. Smith, A. M. Soderberg, A. L. Spadafora, L. . Strolger, M. Strovink, N. B. Suntzeff, N. Suzuki, R. C. Thomas, N. A. Walton, L. Wang, W. M. Wood-Vasey, and J. L. Yun, *Improved Cosmological Constraints from New, Old and Combined Supernova Datasets*, *ArXiv e-prints* **804** (2008) [[arXiv:0804.4142](#)].
- [31] J. Dunlop, J. Peacock, H. Spinrad, A. Dey, R. Jimenez, D. Stern, and R. Windhorst, *A 3.5-Gyr-old galaxy at redshift 1.55*, *Nature* **381** (1996) 581.
- [32] H. Spinrad, A. Dey, D. Stern, J. Dunlop, J. Peacock, R. Jimenez, and R. Windhorst, *LBDS 53W091: an Old, Red Galaxy at  $z=1.552$* , *Astrophys. J.* **484** (1997) 581.
- [33] L. L. Cowie, A. Songaila, and A. J. Barger, *Evidence for a Gradual Decline in the Universal Rest-Frame Ultraviolet Luminosity Density for  $Z < 1$* , *Astron. J.* **118** (1999) 603.
- [34] A. Heavens, B. Panter, R. Jimenez, and J. Dunlop, *The star-formation history of the Universe from the stellar populations of nearby galaxies*, *Nature* **428** (2004) 625.
- [35] D. Thomas, C. Maraston, R. Bender, and C. Mendes de Oliveira, *The Epochs of Early-Type Galaxy Formation as a Function of Environment*, *Astrophys. J.* **621** (2005) 673.
- [36] T. Treu, R. S. Ellis, T. X. Liao, P. G. van Dokkum, P. Tozzi, A. Coil, J. Newman, M. C. Cooper, and M. Davis, *The Assembly History of Field Spheroidals: Evolution of Mass-to-Light Ratios and Signatures of Recent Star Formation*, *Astrophys. J.* **633** (2005) 174.
- [37] B. Panter, R. Jimenez, A. F. Heavens, and S. Charlot, *The star formation histories of galaxies in the Sloan Digital Sky Survey*, *MNRAS* **378** (2007) 1550.
- [38] A. Stockton, M. Kellogg, and S. E. Ridgway, *The nature of the stellar continuum in the radio galaxy 3C 65*, *Astrophys. J. L.* **443** (1995) L69.
- [39] A. Stockton, *The Oldest Stellar Populations at  $z \sim 1.5$* , in *Astrophysical Ages and Times Scales* (T. von Hippel, C. Simpson, & N. Manset, ed.), vol. 245 of *Astrophysical Ages and Times Scales*, *ASP Conference Series*, p. 517, 2001.
- [40] J. S. Alcaniz and J. A. S. Lima, *Dark Energy and the Epoch of Galaxy Formation*, *Astrophys. J. L.* **550** (2001) L133.
- [41] R. Jimenez, L. Verde, T. Treu, and D. Stern, *Constraints on the Equation of State of Dark Energy and the Hubble Constant from Stellar Ages and the Cosmic Microwave Background*, *Astrophys. J.* **593** (2003) 622.
- [42] J. Simon, L. Verde, and R. Jimenez, *Constraints on the redshift dependence of the dark energy potential*, *Physical Review D* **71** (2005), no. 12 123001.
- [43] D. Stern, R. Jimenez, L. Verde, M. Kamionkowski, and S. A. Stanford, *Cosmic chronometers: constraining the equation of state of dark energy. I:  $H(z)$  measurements*, *Journal of Cosmology and Astro-Particle Physics* **2** (2010) 8, [[arXiv:0907.3149](#)].
- [44] A. Sandage, *The Change of Redshift and Apparent Luminosity of Galaxies due to the Deceleration of Selected Expanding Universes.*, *Astrophys. J.* **136** (1962) 319.

- [45] C. Bonvin, R. Durrer, and M. Kunz, *Dipole of the Luminosity Distance: A Direct Measure of  $H(z)$* , *Physical Review L* **96** (2006) 191302.
- [46] E. Gaztañaga, A. Cabré, and L. Hui, *Clustering of luminous red galaxies - IV. Baryon acoustic peak in the line-of-sight direction and a direct measurement of  $H(z)$* , *MNRAS* **399** (2009) 1663, [[arXiv:0807.3551](#)].
- [47] J. Miralda-Escude, *Comment on the claimed radial BAO detection by Gaztanaga et al*, *ArXiv e-prints* (2009) [[arXiv:0901.1219](#)].
- [48] A. Cabre and E. Gaztañaga, *Have Baryonic Acoustic Oscillations in the galaxy distribution really been measured?*, *ArXiv e-prints* (2010) [[arXiv:1011.2729](#)].
- [49] A. G. Riess, L. Macri, S. Casertano, M. Sosey, H. Lampeitl, H. C. Ferguson, A. V. Filippenko, S. W. Jha, W. Li, R. Chornock, and D. Sarkar, *A Redetermination of the Hubble Constant with the Hubble Space Telescope from a Differential Distance Ladder*, *Astrophys. J.* **699** (2009) 539, [[arXiv:0905.0695](#)].
- [50] K. Glazebrook and C. Blake, *Measuring the Cosmic Evolution of Dark Energy with Baryonic Oscillations in the Galaxy Power Spectrum*, *Astrophys. J.* **631** (2005) 1.